A&A 379, 1138–1152 (2001)
DOI: 10.1051/0004-6361:20011405

Astronomy & Astrophysics

Formation of a proto-quasar from accretion flows in a halo

A. Mangalam⋆

Indian Institute of Astrophysics, Koramangala, Bangalore 560034, India

Received 23 April 2001 / Accepted 4 October 2001

Abstract. We present a detailed model for the formation of massive objects at the centers of galaxies. The effects of supernovae heating and the conditions of gas loss are revisited. The escape time of the gas is compared with the cooling time, which provides an additional condition not previously considered. Its consequences for the allowed mass range of the halo is calculated and parameterized in terms of the spin parameter, $\lambda_{\rm v}$, the redshift of collapse, $z_{\rm c}$, the fraction of baryons in stars, f_*, and the efficiency of supernovae, ν. It is shown that sufficient gas is retained to form massive dark objects and quasars even for moderately massive halos but a decline is expected at low redshifts. Subsequently, a gaseous disk forms with a radial extent of a kpc, spun up by tidal torques and magnetized by supernovae fields with fields strengths of 10–100 μG. In a model of a self-similar accretion flow in an initially dominant halo, it is shown that for typical halo parameters, about 10^8 $M_\odot$ accretes via small magnetic stresses (or alternatively by self-gravity induced instability or by alpha viscosity) in 10^8 years into a compact region. A model of a self-gravitating evolution of a compact magnetized disk ($r_0 \lesssim 100$ pc), which is relevant when a significant fraction of the disk mass falls in, is presented, and it has a rapid collapse time scale of a million years. The two disk solutions, one for accretion in an imposed halo potential and the other for a self-gravitating disk, obtained here, have general utility and can be adapted to other contexts like protostellar disks as well. Implications of this work for dwarf galaxy formation, and a residual large scale seed field, are also breifly discussed.

Key words. accretion, accretion disks – magnetic fields – galaxies: formation – cosmology: theory

1. Introduction

There seems to be increasing evidence that supermassive black holes are at the centers of galaxies. Dynamical searches indicate the existence of massive dark objects (MDOs) in eight systems and their masses range from 10^6–$10^{9.5}$ $M_\odot$ (Kormendy & Richstone 1995). Although this study does not confirm that the central objects are supermassive black holes, it has been inferred that the central mass is contained within 10^5 Schwarzchild radii. On an average, the black hole mass is a fraction, 10^{-2}–10^{-3}, of the total mass of the galaxy and of order $10^{-3.5}$ of the bulge mass (Wandel 1999). Recent observations show a strong correlation between the black hole mass, $\mathtt{m}_{\rm h}$, from stellar dynamical estimates, and the velocity dispersion of the host bulges ($\mathtt{m}_{\rm h} \propto \sigma^\alpha$; where α is reported to be in the range 3.5–5; e.g. Ferrarese & Merritt 2000). This has been supported by reverberation mapping studies of the broad line region (Gebhardt et al. 2000). The black hole masses in active galaxies as inferred from their luminosities, assuming reasonable efficiencies, are also in the same range, 10^{6-10} $M_\odot$. Arguments based on time variability, relativistic jets and other circumstantial evidence indicate that they are relativistically compact (Blandford & Rees 1992). Specific examples include a $\sim$20 pc disk spining at 500 km s^{-1} which implies a 2×10^9 $M_\odot$ black hole in M 87 (Ford et al. 1994) and evidence of 10^7 $M_\odot$ mass in a region of 0.1 pc in the case of NGC 4258 (Miyoshi et al. 1995). One remarkable fact is that there is a decline in the quasar population between $z = 2$ and the present epoch. The presence of quasars at high redshifts tells us that galaxy formation had proceeded far enough for supermassive black holes to form in the standard picture (Rees 1984). A detailed model of formation of these objects, such as the one attempted here, should address the issues of supernovae feedback from star formation and the mechanism of efficient angular momentum transport in order to explain the massive active nuclei as early as $z = 5$. In the case of MDOs, there is a need to explain the compact sizes of 10–100 pc that are implied from dynamical studies.

Broadly, the two main routes to the formation of the massive central objects that have been proposed are through instabilities in a relativistic stellar cluster or gas dynamical schemes which may involve a direct collapse of a primordial gas cloud or accretion of a collapsed gaseous disk. The main drawback of the stellar cluster models is that one must assume the existence of a dense and massive cluster at the outset; the angular momentum transport

⋆ e-mail: mangalam@iiap.ernet.in

problem to arrive at this initial scenario is difficult to overcome. One gas dynamical scheme proposed by Shlosman et al. (1990) involves accretion of gas through stellar bars which have been induced either by self-gravity or galaxy interactions driving the gas from 10 kpc to about a kpc size "disk of clouds" which further accretes by viscous dissipation due to cloud-cloud collisions. N-body simulations (Sellwood & Moore 1998) have shown that the bar weakens substantially after a few percent of the disk mass accumulates in the center. This mechanism may not last long enough to drive sufficient matter into a compact region as the bar instability is suppressed by the bulge at the inner Linblad resonance. Disk accretion due to self-gravity and magnetic fields may then be better candidates to transport the mass to about a 100 pc size compact region.

Loeb & Rasio (1994) considered the possibility that massive black holes form directly during the intial collapse of the protogalaxies at high redshifts and performed smoothed particle hydrodynamical simulations of gas clouds. They find that inital collapse of a protogalactic cloud leads to the formation of a rotatinally supported thin disk. They argue that if the viscous transport time in the disk is small compared to the cooling time, then the disk could collapse to a supermassive star, else it could form a supermassive disk; they do not provide gas dynamical collapse model after the formation of a disk or star. They found that the gas fragments into small dense clumps (presumably are converted into stars). The important consequences of supernovae feedback is not considered. Eisentein & Loeb (1995) suggest that quasars may be associated with rare systems that acquire low values of angular momentum from tidal torques during the cosmological collapse. Typically these are 10^5 $M_\odot$ objects and form at redshifts $z \gtrsim 10$. Since the viscous evolution times in the collapsed disks of these objects are comparable to star formation times, it is important to consider the effects of supernovae feedback in detail that could disrupt these objects.

Natarajan (1999) considers the effect of feedback and argues that the fraction of the gas retained is proportional to ratio of the supernovae heat input to the binding energy of the gas in the halo. This assumption has interesting consequences for the Tully-Fisher relationship. The criteria for mass loss was considered by Mac-Low & Ferrara (1999), Ferrara & Tolstoy (2000) in the context of a blow-out or a blow-away (when the mass is completely expelled) from disk galaxy with an isothermal atmosphere. The condition for the gas to be retained is that the blow-out velocity be less than the escape velocity. However, the cooling of the hot gas is not considered. In this paper, we consider the possibility that gas cools before it escapes the halo.

Silk & Rees (1998) propose that $\sim 10^5$ $M_\odot$ clouds at high redshifts undergo direct collapse in a hierarchical (bottom-up) CDM cosmology without undergoing fragmentation and star formation arguing that the conditions in primordial clouds differ from conventional molecular clouds. The angular momentum in this picture is shed by non-axisymmetric gravitational instabilities. The more

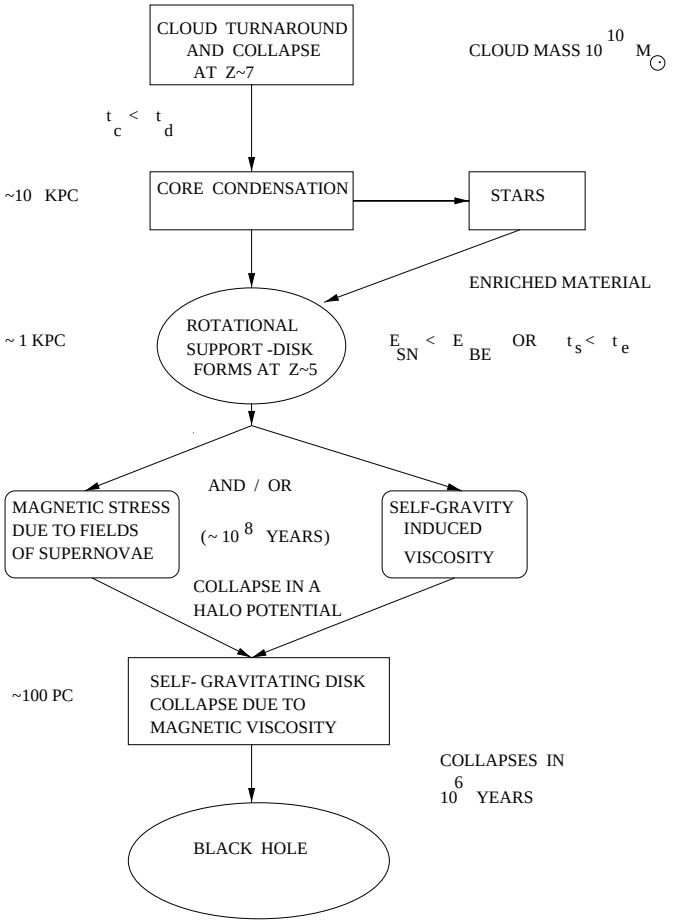

Fig. 1. The evolution of a 10^{10} $M_\odot$ cloud leading to a formation of a protoquasar. In first step, this cloud cools faster than the dynamical time, $t_\mathrm{c} < t_\mathrm{d}$. After star formation, one of the conditions is satisfied- that the supernovae heat energy is less than the binding energy, $E_\mathrm{SN} < E_\mathrm{BE}$ or that the cooling time of the hot gas is less than the time to escape the halo, $t_\mathrm{s} < t_\mathrm{e}$.

massive black holes (10^7 $M_\odot$) ejects mass from the host galaxies by assumed spherical quasar winds. In the limiting case, it provides a relationship between the mass of the central hole and the host galaxy mass. The time between halo virialization and the birth of quasars is short compared to the cosmological timescale. Haehnelt & Rees (1993) proposed a scenario in which a disk forms (after turnaround and collapse) and loses angular momentum due to α viscosity in an estimated timescale of 10^8 yrs.

Here, we discuss a detailed physical model for the formation of protoquasars (or MDOs) from a magnetized accretion of a collapsed disk, the properties of which are obtained taking into account supernovae feedback in a virialized halo. There is observational evidence that considerable fragmentation precedes quasar activity and the broad emission lines in quasar spectra indicate high metallicity (Hamann & Ferland 1992). We assume, therefore, significant star formation and supernovae activity occurs after the cloud, which is spun up by tidal torques, contracts to a radius where self-gravity is significant. The paper is composed of the following parts (see Fig. 1).

1. The formation of a gaseous disk with a radial extent of about a kpc, in a host galaxy as limited by supernovae feed back. We investigate in Sect. 2, the range in halo mass for a given redshift that still retains the hot gas. The effect of the evolution of gas on the collisionless dark matter system is neglected;
2. In previous work, gravitational instabilities (examined in Sect. 4.3) in the disk was considered as the main source of viscosity. In Sect. 4.1, justification is made for a magnetic viscosity from supernovae fields and the estimated accretion rate turns out to be significant; also the large scale field strength derived from the effective seed of small scale fields is used to explain observations (Sect. 3);
3. The collapse of the disk is calculated with a generalized viscosity prescription (which includes the individual cases of magnetic, α and self-gravity induced instabilities, Sect. 4) under a halo dominated gravitational potential (Sect. 5) into a compact central region at rapid rate of about a $M_\odot$ yr^{-1}. A self-gravitating magnetized disk solution for this central object that collapses in 10^6 yrs, is presented in Sect. 6. There is summary and discussion in Sect. 7 and conclusions in Sect. 8.

2. The virialized spherical halo and formation of the gaseous disk

We assume a standard spherical model for the formation of a virialized spherical halo to begin with, in which the gas cools to form the disk. Subsequently, we include in the calculations the supernovae heating and consider the conditions under which sufficient gas is retained to form the disk.

A particularly simple and useful version of the spherical model below assumes that the matter distribution is symmetric about a point and is a pressureless fluid. The shell enclosing mass of the overdense region, $\mathcal{M}$, initially expands with the background universe, slows down, reaches a maximum radius before it turns around, and collapses. The collapse proceeds until a time when it reaches virial equilibrium. For an average density contrast, δ, and using the fact that the background density, $\rho_{\rm b} \propto t^{-2}$ for a flat cosmological model, one can make the following estimates of the typical parameters of the collapsed object (Padmanabhan & Subramanian 1992; Padmanabhan 1993; Peebles 1980)

$$\begin{aligned}
\rho_0 &= 9.1\times10^{-30}\ \Omega\ h_{70}^2\ \text{g cm}^{-3}\\
\tau_0 &= 0.94\times10^{10}\ h_{70}^{-1}\ \text{yr}\\
r_{\rm v} &= r_{\rm t}/2 = (78/\delta_0)\ \mathcal{M}_{10}^{1/3}\ h_{70}^{-2/3}\ \text{kpc}\\
\tau_{\rm c} &= 2.19\ \tau_0/\delta_0^{2/3}\\
\delta_0 &= (3\pi/2)^{3/2}\ (1+z_{\rm c}) = 1.686\ (1+z_{\rm c}) = 1.062\ (1+z_{\rm t}),
\end{aligned} \tag{1}$$

where ρ_0 and τ_0 are the current values of the comoving density and time, the subscripts t and c indicate turn around and collapse values, and $r_{\rm v}$ is the radius of virialization. For a given model of the cosmological evolution of the initial density perturbation, one obtains values for δ_0 or alternatively one can specify the collapse redshift. As an example, $z_{\rm t} = 6.3$ corresponds to $z_{\rm c} = 3.6$ and a $\delta_0 = 7.8$. We take $\Omega_{\rm b} = 0.1\ h_{70}^{-2}$ and the mass in baryons, M_9, in units of $10^9\ M_\odot$, is related to the total mass by

$$M_9 = \frac{h_{70}^{-2}}{\Omega}\ \mathcal{M}_{10} \equiv \frac{f_{\rm b}}{0.1}\ \mathcal{M}_{10}. \tag{2}$$

The baryonic mass, M_9, will fuel a black hole, after it has formed, at a rate limited by the Eddington luminosity. If the accretion proceeds at a tenth of this rate, then the luminosity in units of 10^{45} ergs s^{-1} is

$$L_{45} = 1.3\ \mathtt{m}_{\rm h8}, \tag{3}$$

where $\mathtt{m}_{\rm h8}$ is the mass of the black hole in units of $10^8\ M_\odot$.

2.1. Calculation of the collapse factor $r_{\rm v}/r_{\rm d}$

The gas in the massive dark halo of size $r_{\rm v}$ radiative cools to form a disk of radial extent $r_{\rm d}$. Before we consider the details of cooling in Sect. 2.2, we first need to estimate the collapse factor, $r_{\rm v}/r_{\rm d}$, which is based upon the conservation of angular momentum. The disk forms when the gas becomes rotationally supported. The protoquasar acquires its spin from tidal torques of its neighbors and N-body simulations (Barnes & Efsthaiou 1987) and analytical studies (Heavens & Peacock 1988) indicate that the spin parameter of the virialized system, $\lambda_{\rm v}$, to be in the range 0.01–0.1. If the angular momentum is conserved and there is no exchange between the gas and dark components, the ratio of angular momentum in the gas to the halo would remain as $M_{\rm d}/\mathcal{M}$, so that

$$\frac{\lambda_{\rm d}}{\lambda_{\rm v}} = \left(\frac{E_{\rm d}}{E}\right)^{1/2}\ \left(\frac{\mathcal{M}}{M_{\rm d}}\right)^{3/2} \tag{4}$$

where $\lambda \equiv L|E|^{1/2}/GM^{5/2}$ is the spin parameter, L is the angular mometum, and $E = -k_1 G\mathcal{M}^2/r_{\rm v}$ and $E_{\rm d} = -k_2 GM_{\rm d}^2/r_{\rm d}$ are the binding energies in the halo and the disk respectively. If the halo has a constant density then $k_1 = 0.3$ and if it were a truncated isothermal sphere then $k_1 = 0.5$. Using the form for the circular velocity, $v_{\rm c} = \sqrt{G\mathcal{M}/r_{\rm v}}$, of a disk spinning in an isothermal halo and taking the angular momentum of the disk to be equal to $sM_{\rm d}r_{\rm d}v_{\rm c}$, where s is a geometrical factor (typically of order unity; $s = 2$ for an exponential disk) that depends on the mass distribution in the disk, the radial extent of the disk is given by

$$r_{\rm d} = r_{\rm v}\ \left(\frac{1}{s\sqrt{k_1}}\right)\ \lambda_{\rm v}. \tag{5}$$

Typically, the disk size is a tenth of the virial radius, and the collapse factor ranges from 10 to 20. For convenience we make the following definitions

$$x_{\rm v} = \frac{r_{\rm v}}{10\ \text{kpc}} \tag{6}$$

$$x_{\rm d} = \frac{r_{\rm d}}{1\ \text{kpc}} \tag{7}$$

where $r_{\rm d}$ is the radius of the disk.

2.2. Cooling

In order that gaseous disks (with collapse factor estimated above) form in the halo where star formation and supernovae take place, it is important to examine whether the gas can be retained in the hosts in the first place. In this section, we examine the constraints on black hole hosts (those that can retain the gas) from star formation and gas loss due to supernovae. Consider a virialized halo which contracts due to cooling to a radius where it fragments due to self-gravity and star formation takes place. Below we list the conditions that specify when a halo condenses to form stars, whether the gas becomes unbound due to supernovae heating and finally whether the gas cools before it can escape and hence remains trapped in the halo. The first two of the conditions were considered earlier and in this paper we introduce a third necessary condition previously not considered.

C0. Following earlier work (e.g. White & Rees 1979; Rees & Ostriker 1977; Silk 1977), we state the condition that a luminous core can form in a halo

$$t_{\rm c} < t_{\rm d} \tag{8}$$

where $t_{\rm c}$ is the cooling time and $t_{\rm d}$ is the dynamical time. The heating process by was examined in some detail by Dekel & Silk (1986, DS) in the context of dwarf galaxies; they found that a condition of gas loss amounted to the virial velocity being below a certain critical velocity. At a time, $t_{\rm f}$, when the hot gas in supernovae shells significantly fills up the volume under consideration, the following constraints should be satisfied.

C1. As given by DS, the effective heat input by supernovae is

$$E_{\rm sn}(t_{\rm f}) \geq \frac{1}{2} f_{\rm g} \mathcal{M} v_{\rm c}^2 \tag{9}$$

where $f_{\rm g}$ is the gas fraction in the total mass and $v_{\rm c}$ is the circular (or virial) velocity in the halo. This implies that the supernovae heat input should be greater the binding energy for the gas to escape.

C2. We find that an additional condition for gas loss is necessary, namely, that the time for the hot gas to cool should be longer than the escape time, $t_{\rm e}$ of the system

$$\frac{E_{\rm sn}}{\dot{E}} > t_{\rm e}, \tag{10}$$

where $t_{\rm e}$ is approximated by the time scale

$$t_{\rm e} = \int_0^{r_{\rm v}} \frac{{\rm d}r}{\sqrt{2(\overline{E} - \Phi)}}, \tag{11}$$

where $\overline{E}$ represents the mean kinetic energy per unit mass and Φ is the mean gravitational potential per unit mass. In other words, even if supernovae heat input causes the gas to become unbound, it can still be trapped in the halo if it cools faster than the time required to escape, which is of the order of the dynamical time.

In order to quantify these physical constraints, we have to calculate $E_{\rm sn}$, the effective heat input by supernovae. The standard evolution of a supernova remnant goes through two phases- adiabatic and radiative. In the adiabatic phase (Sedov-Taylor), the radiation loss is negligible and the time at which the shock front radiates about three-quarters of its initial energy is given by DS as

$$t_{\rm rad} \approx 1.4 \times 10^5 \; n^{-1/2} \; {\rm yr}, \tag{12}$$

where n is the ambient hydrogen number density in ${\rm cm}^{-3}$. As a result, the input into the gas equals the initial energy minus the radiative losses in the adiabatic phase and subsequently for later times, the gas is cooled by expansion. The cumulative energy input from the supernovae at a given time, t, will be dominated by those that have exploded within a time $t_{\rm rad}$ before t. The star formation rate is taken to be a constant and is approximately, $f_* M/t_{\rm d}$, where f_* is the baryonic mass fraction in stars and further, it is assumed that the star formation abruptly ends at $t = t_{\rm d}$. The IMF of the solar neighborhood gives rise to one supernova per 200 $M_\odot$ of newly formed stars. If ν_{200} is the number of supernova explosions per 200 $M_\odot$ of newly formed stars[1] with each explosion releasing $\epsilon_0 = 10^{51}$ ergs of initial energy, then the energy input into the gas is then given by

$$E_{\rm sn}(t) = \epsilon_0 \; f_* \; \frac{M}{200 \; M_\odot} \; \nu_{200} \; \frac{t_{\rm rad}}{t_{\rm d}} \; f(t) \tag{13}$$

and the dynamical time for the system is a quarter of the oscillation period given by

$$t_{\rm d} = \frac{\pi}{2} \sqrt{\frac{r_{\rm v}^3}{G\mathcal{M}}} = 4.5 \times 10^8 \; \mathcal{M}_{10}^{-1/2} \; x_{\rm v}^{3/2} \; {\rm yrs}, \tag{14}$$

which is assumed to set the timescale for star formation. Also, $f(t)$, is a function of time that is of order unity and its form is given by Eq. (45) in DS

$$f(t) = \begin{cases} (t/t_{\rm rad})[1 - 0.14(t/t_{\rm rad})^{17/5}] & t \leq t_{\rm rad} \\ 0.86 + 0.58[(t/t_{\rm rad})^{0.38} - 1] & t > t_{\rm rad}. \end{cases} \tag{15}$$

The ratio $t_{\rm rad}/t_{\rm d} \approx 0.01 \; \sqrt{f_{\rm b}/0.1}$ implies that $f(t)$ is of order unity and $0 < f(t) < 3.6$ (for $0 < t < t_{\rm d}$). The heat input from the supernovae that have exploded within a time, $t_{\rm rad}$, of a given instant are the most effective in contributing to the heating. Now the shells of the supernovae will start filling up the volume. The time at which hot gas has a filling factor of order unity ($t = t_{\rm f}$), is estimated in the following manner.

[1] An analytic fit to the IMF (Eq. (1.3.10), Shapiro & Teukolsky 1983) which is based on Bahcall & Soniera (1980), yields the ratio of the number of objects in the mass range $5 < M/M_\odot < 30$ to the total mass in all the stars (with a cutoff at 0.1 $M_\odot$) to be 5×10^{-3} per solar mass; this we have adopted as a fiducial value of the number of supernovae per solar mass of newly formed stars.

2.3. Filling factor of SNR

We use the well-known simple expressions (e.g. Spitzer 1978) for the advance of the supernova through the Sedov-Taylor and snow-plow phases in a medium whose number density of hydrogen is typically $n = (1/130)(\mathcal{M}_{10}/x_{\rm v}^3) = (1/130)(\frac{4.6}{1+z_{\rm c}})^3$, which is in the range of 0.01 to 1 H atom cm^{-3}. In the Sedov-Taylor phase, during which the total energy in shock front is conserved, the advance of the shock front is given by

$$r_{\rm st} = 10^{15}\ t^{2/5}\ n^{-1/5}\ {\rm cm}, \tag{16}$$

where t is seconds. This phase ends when the temperature falls below 10^6 K and radiative losses are significant at a time $t_{\rm rad}$, given by Eq. (12). The radius at beginning of the radiative phase as given by this condition is then

$$r_{\rm rad} = n^{-2/5}\ 40\ {\rm pc}. \tag{17}$$

Next, the radiative (snow-plow) phase follows, in which the momentum is roughly conserved and the shock front advances according to $r_{\rm s} \propto t^{0.31}$ (Chevalier 1974). The star formation is expected to occur when the gas in the halo shrinks to some size R ($\sim f_{\rm b} r_{\rm v}$ if it is isothermal or $\sim f_{\rm b}^{1/3} r_{\rm v}$ if the gas cloud is uniform) and fragments due to self-gravity (Larson 1974). Taking the typical size of the remnant as given by Eq. (17), the total shell volume of the supernovae remnants in units of the volume occupied by the gas is

$$\begin{aligned} F(t) &= \frac{t}{t_{\rm d}}\ \frac{r_{\rm rad}^3\ \nu_{200}\ f_*(M/200\ M_\odot)}{R^3} \\ &\simeq 10\ \frac{4f_*}{1-f_*}\ \nu_{200}\ n^{-1/5}\ \frac{t}{t_{\rm d}}, \end{aligned} \tag{18}$$

where Eq. (17) and the density of the gas, $M(1-f_*)/(4\pi R^3/3) = 1.4\ n\ m_{\rm p}$ was used. Since the star formation shuts off at $t = t_{\rm d}$, the maximum value of the ratio of the total shell volume to gas volume is $F(t > t_{\rm d}) = 10\ (4f_*/(1-f_*))\ \nu_{200}\ n^{-1/5}$. This implies that the filling factor of the supernovae shells in the galaxy will be weakly dependent on number density. One can take into account the porosity (which can be thought of as the complement of the probability that a given point in the volume is outside the $N = \nu_{200}\ f_*\ M_9\ (5\times10^6)$ remnants of fractional volume, $q = F(t)/N$, occupied by one shell) by $Q = 1-(1-q)^N$, where Q is the filling factor, which is well approximated in the Poisson limit of large N by the formula,

$$Q(t) = 1 - \exp\left(-F(t)\right). \tag{19}$$

It is clear that Q at large times is close to 1 (and nearly independent of density) and the hot gas fills the volume. In order to estimate the total energy input into the medium in Eq. (13), we calculate the time, $t_{\rm f}$, when $Q \approx 1, F(t_{\rm f}) = 3$ which leads to $t_{\rm f} = F(t_{\rm f})t_{\rm d}/F(t_{\rm d}) \simeq 0.3t_{\rm d} = 30\ t_{\rm rad}$.

2.4. Gas loss criteria

The solution leads to $f(t_{\rm f}) \approx 3$, from Eq. (15). So the energy input into gas from supernovae works out to be

$$E_{\rm sn}(t_{\rm f}) = 3\times10^{55}\ \frac{f_*}{0.2}\ \frac{f_{\rm b}}{0.1}\ \nu_{200}\ \mathcal{M}_{10}\ {\rm ergs}. \tag{20}$$

The escape energy is given by

$$\begin{aligned} \frac{1}{2}\ f_{\rm g}\ \mathcal{M}\ v_{\rm c}^2 &= \frac{1}{2}\ \frac{G f_{\rm g}\mathcal{M}^2}{r_{\rm v}} \\ &= 4\times10^{55}\ \frac{(1-f_*)}{0.8}\ \frac{f_{\rm b}}{0.1}\ \frac{\mathcal{M}_{10}^2}{x_{\rm v}}\ {\rm ergs} \end{aligned} \tag{21}$$

where

$$v_{\rm c} = 0.7\times10^7\sqrt{\mathcal{M}_{10}/x_{\rm v}}\ {\rm cm\ s^{-1}} \tag{22}$$

is the virial velocity. As a result the condition C1 for gas removal can be written as

$$\frac{v_{\rm sn}^2}{v_{\rm c}^2} = \frac{3f_*}{1-f_*}\ \frac{x_{\rm v}}{\mathcal{M}_{10}}\ \nu_{200} > 1 \tag{23}$$

where $v_{\rm sn}^2 = 2E_{\rm sn}/(f_{\rm g}\mathcal{M})$ where $f_{\rm g} = 1 - f_{\rm b}(1-f_*)$ is the gas fraction in the halo mass not converted to stars. It is clear that enhancing the star fraction increases the energy input into a smaller gas fraction and hence $v_{\rm sn}^2$ is a monotonically increasing function of f_*. Also, halos of the same mass had deeper potential wells in the past which trap the gas better. Similarly, more massive halos clearly have deeper wells and gas loss is less likely as seen from Eq. (23).

In Appendix A, we calculate the difference in gravitational binding energies in the initial configuration of an isothermal halo and a final one consisting of an exponential gaseous disk in a halo consisting of stars and dark matter. The gas taken to be roughly near the virial temperature,

$$T_{\rm v} = \frac{G\ \mathcal{M}\ \mu\ m_{\rm p}}{3\ k_{\rm b}\ r_{\rm v}} = \frac{\mathcal{M}_{10}}{x_{\rm v}}\ 10^5\ {\rm K} \tag{24}$$

where the mean molecular weight, $\mu = 0.6$. The cooling proceeds through line and free-free emission and we take a cooling function, $\Lambda(T) = 10^{-23}$ ergs s^{-1} cm^{-3} $\Lambda_{23}(T)$, provided by Sutherland & Dopita (1993) for a metallicity of [Fe/H] $= -4$. The cooling rate in the virialized halo during the contraction is roughly given by

$$\dot{E}_{\rm h} = \Lambda\ n_{\rm e}\ N_{\rm e} = 4.5\times10^{41}\ \Lambda_{23}(T_{\rm v})\ M_9^2\ x_{\rm v}^{-3}\ {\rm ergs\ s^{-1}}, \tag{25}$$

where $N_{\rm e}$ is the number of electrons. Now, we can estimate the cooling time taken for the system to cool and fragment, given that the source of thermal energy in the gas is one-half the change in gravitational potential energy from the virial theorem. The cooling time, $t_{\rm c}$, is given by

$$t_{\rm c} = \frac{\Delta W/2}{\dot{E}_{\rm h}(T_{\rm v})} \tag{26}$$

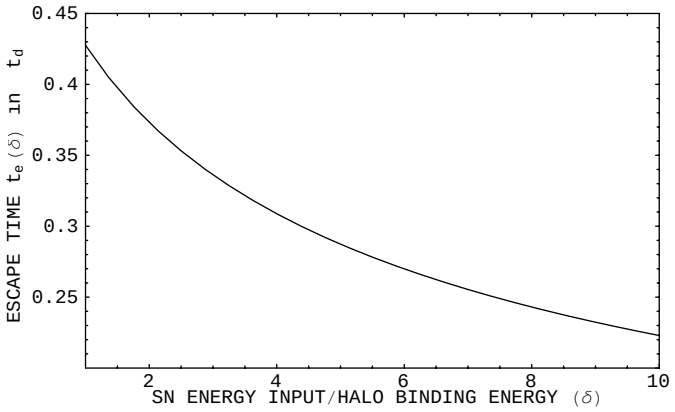

Fig. 2. The dependence of the escape time of the hot gas, in units of the dynamical time in the halo which is defined as one-quarter oscillation period, on $\delta = v_{\rm sn}^2/v_{\rm c}^2$, the supernovae energy input in units of the halo binding energy. A factor of 10 in the heat input reduces the escape time, $t_{\rm e}$, by factor of 2.

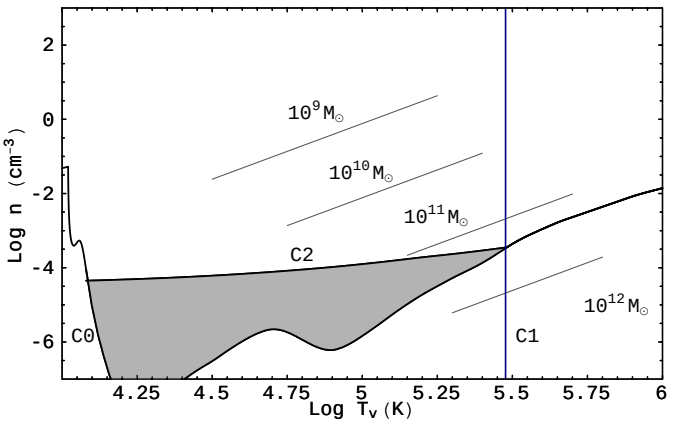

Fig. 3. The shaded region bounded by the constraints, C0, C1, and C2 in the cooling diagram contains the halos that have cooled and contracted to a radius of fragmentation; however, the supernovae heated gas in these systems have escape times shorter than the cooling time, resulting in gas-poor galaxies. The parameters chosen here are $f_* = 0.2, \nu_{200} = 4$, and $\lambda_{\rm v} = 0.075$. The halos above C2 for $\delta > 1$ (on the left of C1) and above C0 for $\delta < 1$ can trap the gas and hence are the candidate hosts of central massive objects.

where $T_{\rm v} = 10^5 \mathcal{M}_{10}/x_{\rm v}$ and plugging in the expressions for ΔW from Appendix A, the condition of core condensation C0, thus, can be expressed as

$$\left(\frac{0.08}{f_{\rm g}}\right) \frac{\sqrt{\mathcal{M}_{10} x_{\rm v}}}{94} \left[\frac{0.3}{\lambda_{\rm v}} - \frac{1}{2}\right] \Lambda_{23}(T_{\rm v})^{-1} < 1. \quad (27)$$

After fragmentation and star formation, the gas is heated up and the hot gas cools in a time, $t_{\rm s} = E_{\rm sn}/\dot{E}(T_{\rm sn})$ where $T_{\rm sn} = v_{\rm sn}^2 \mu m_{\rm p}/(3k_{\rm b}) = \delta\, T_{\rm v} = 10^5\, \delta\, \mathcal{M}_{10}/x_{\rm v}$ is the temperature of the heated gas and $\delta = v_{\rm sn}^2/v_{\rm c}^2 = (x_{\rm v}\nu_{200}/\mathcal{M}_{10})\, 3f_*/(1-f_*)$. Now, we need to compare this to the escape time, as defined in Eq. (11), when the condition C1 is satisfied or a quarter of the oscillation period when the system is bound. Now, $\overline{E} = E_{\rm sn}/(f_{\rm g}M) - v_{\rm c}^2/2 = v_{\rm c}^2(\delta-1)/2$, is the mean energy of a gas particle in the system and is zero when the escape velocity equals the critical velocity. Using the potential for an isothermal sphere that is truncated at $r_{\rm v}$, $\Phi(r < r_{\rm v}) = v_{\rm c}^2(\ln(r/r_{\rm v}) - 1)$, and $r_{\rm v}/v_{\rm c} = (2/\pi)t_{\rm d}$, we obtain

$$t_{\rm e}(\delta) = t_{\rm d}\sqrt{\frac{2}{\pi}} \exp\left(\frac{1+\delta}{2}\right) \times \left[1 - {\rm Erf}\left(\sqrt{\frac{1+\delta}{2}}\right)\right] \quad \delta \geq 1 \quad (28)$$

which is valid for $\delta > 1$, for which the supernova heat input, $E_{\rm sn}$, is such that the resulting mean energy of the particles is positive. These particles can escape only if the cooling time is longer than the escape time. The escape time, $t_{\rm e}(\delta)$, is a slowly decreasing function and is of order $t_{\rm d}$ (See Fig. 2). For $\delta < 1$, the gas remains bound and only the condition of core condensation, C0, applies. Hence, the condition C2, $t_{\rm s}/t_{\rm e} > 1$, can be expressed as

$$\left(\frac{0.08}{f_{\rm g}}\right) \frac{\sqrt{\mathcal{M}_{10} x_{\rm v}}}{94}\, \delta\, \Lambda_{23}(T_{\rm sn})^{-1} \frac{0.418\, t_{\rm d}}{t_{\rm e}(\delta)} > 1, \quad (29)$$

where the effective dynamical timescale at $\delta = 1$ is taken to be $t_{\rm d}$ and $t_{\rm e}(1) = 0.418\ t_{\rm d}$, so that the curve C2 is continuous with C0. This is seen in the cooling diagram, presented in Fig. 3, where the number density of hydrogen in the halo, $n({\rm cm}^{-3}) = \mathcal{M}_{10}/(130 x_{\rm v}^3)$, is plotted against the virial temperature, $T_{\rm v}$ and shows the curves given by C0, the lower curve, C1, the vertical line, and C2 which is the upper curve in the region to the left of C1. The cosmological parameters were set to $h_{70} = 1, \Omega = 1$, and $f_{\rm b} = 0.1$ and the halo parameters were chosen to be $\lambda_{\rm v} = 0.075, f_* = 0.2$, and $\nu_{200} = 4$. The shaded region indicates the halos that have collapsed but star formation has induced gas loss and they ultimately resulted in gas poor systems. The halos above this region retain the gas that could form the massive central black holes. The corresponding range in mass for a given redshift is shown in Fig. 4, for the choices of the parameters, $\nu_{200} = 4$, the supernova efficiency, and $f_* = 0.2$, the fraction of baryons in stars. Clearly for large redshift, the mass range increases and this is due to the deeper potential well which can retain the gas better. There is a crucial question of whether all the gas is retained or if some fraction is lost in a wind. A supernova efficiency in the halo of

$$\nu_{200}\, \frac{4f_*}{1-f_*} \gtrsim 60\sqrt{\mathcal{M}_{10}/x_{\rm v}^3} = 4.3(1+z_{\rm c})^{3/2}, \quad (30)$$

from Eq. (29), would be required to drive winds that would result in mass loss and this is considerably more than the corresponding estimates in our galaxy, for $z_{\rm c} \gtrsim 2$. If the stars form after the disk forms, the cooling rate in the disk would be given by

$$\dot{E}_{\rm d} = 3{\times}10^{44}\, \Lambda_{23} \left(\frac{f_{\rm b}}{0.1}\right)^2 \mathcal{M}_{10}^2\, x_{\rm d}^{-3} (1-f_*)^2 \frac{r_{\rm d}}{H}\, {\rm ergs\ s^{-1}} \quad (31)$$

and the cooling time would reduce by a factor of a thousand corresponding to enhanced density. Although only

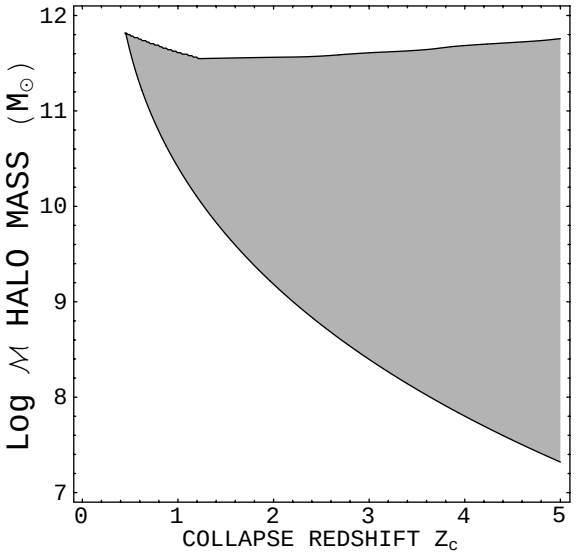

Fig. 4. The halos in the shaded region in the $\mathcal{M}_{10} - z_c$ space can trap the gas; the parameters chosen are $f_* = 0.3, \nu_{200} = 4$, and $\lambda_v = 0.07$.

the cosmological abundance of [Fe/H] $= -4$ was used, the supernovae explosions will also enhance line cooling from metals injected into the medium; this would reduce the cooling time estimated here.

3. Magnetization of the disk

In the large number of the halos which trap the gas as given by the conditions C0–C2, a gaseous disk forms with a radial extent given in Sect. 2.1. Further, it was seen in Sect. 2.3 that the supernovae shells fill the core volume at the time of star formation, and the small scale magnetic fields are dragged with the gas as it settles into a the disk. Now, we consider the question of whether the field strength is large enough to provide a significant viscous stress. We take the gas to be initially dominated by the gravity of the dark halo and assume the following logarithmic potential (Binney & Tremaine 1987, Eqs. (2)–(54)) that obeys the flat rotation curve

$$\Phi(r,z) = v_c^2 \ \ln(r_0^2 + r^2 + (z/q_\phi)^2) \tag{32}$$

where r_0 is the radius of a compact region, $q_\phi \leq 1$ and v_c is defined in Eq. (22). If the vertical equilibrium was a result of balance between vertical gradient in the total pressure, $P = \zeta c_s^2 \rho$ (which represents a sum of magnetic and gas pressures and the density scale height is H), and $-\partial_z \Phi$, we obtain

$$\frac{H}{r} \simeq \sqrt{\zeta} \left(\frac{c_s}{v_c}\right) q_\phi^2. \tag{33}$$

Assuming a dominant isothermal halo, we obtain the half-flaring angle of the disk,

$$\frac{H}{r_d} \simeq \theta \ x_v^{1/2} \mathcal{M}_{10}^{-1/2}, \tag{34}$$

where $\theta = (1/8)\ \sqrt{\zeta}\ (q_\phi^2/0.5)$, and the speed of sound was taken to be $c_s = \sqrt{\frac{\gamma k_B T}{\mu m_p}} = 1.6 \times 10^6$ cm s^{-1} for a temperature of 10^4 K, where the cooling curve drops significantly.

The supernovae inject the medium with magnetic flux and next we estimate the typical strength of the small scale field. The calculation in Sect. 2.3 shows that the filling factor of the shells in the total gas volume is nearly unity for a wide range in density and therefore the supernovae hot gas fills the medium and hence quasi-uniformly magnetizes it. The volume of the flared disk works out to be

$$V_d = \frac{4\pi}{3}\ r_d^2\ H = 1.67 \times 10^8\ \mathrm{pc}^3 (8\,\theta) \times \left(\frac{\lambda_v}{0.075}\right)^3 \left(\frac{4.6}{1+z_c}\right)^3 \mathcal{M}_{10}^{1/2}. \tag{35}$$

The Crab Nebula of size 0.8 pc (or volume 2 pc^3) has 3×10^{-4} G fields (see Sect. 7 for a discussion of supernova field strengths). By freezing the flux in a Crab volume of 2 pc^3 to a volume occupied by one shell, the magnetic field strength in the disk for $N = 10^6 \mathcal{M}_{10} \nu_{200} (f_*/0.2)(f_b/0.1)$ remnants is

$$B_{sn} = 3 \times 10^{-4}\ \mathrm{G}\ \left(\frac{V_d/N}{2\ \mathrm{pc}^3}\right)^{-2/3} = 1.7 \times 10^{-5}\ \mathrm{G}\ \left(\frac{1+z_c}{4.6}\right)^2\ \mathcal{M}_{10}^{1/3} \times \nu_{200}^{2/3}\ \left(\frac{f_*}{0.2}\right)^{2/3}\ \left(\frac{f_b}{0.1}\right)^{2/3}\ \left(\frac{0.075}{\lambda_v}\right)^2. \tag{36}$$

By choosing a typical set of values ($\lambda_v = 0.05, \nu_{200} = 4, f_* = 0.5, \theta = 1/8$) the field strength turns out to be as high as $B_{sn} = 170\ \mu$G.

The mean number density of hydrogen atoms in the flared gaseous disk, for $\mu = 0.6$, is given by

$$n_d = 7.5\ (1 - f_*)\ M_9\ \left(\frac{r_d}{H}\right)\ x_d^{-3} = 150\ \mathrm{cm}^{-3}\ \frac{1-f_*}{0.8}\ \left(\frac{1+z_c}{4.6}\right)^{7/2}\ \mathcal{M}_{10}^{2/3}\ \frac{f_b}{0.1} \tag{37}$$

where (34) and (2) were used and the values of $\lambda_v = 0.075$ and $\theta = 1/8$ were taken. Outflows from O and B stars could also magnetize the gas, and by using flux freezing we estimate the field strength due to winds to be (Bisnovatyi-Kogan et al. 1973; Ruzmaikin et al. 1988)

$$B_w = (\rho/\rho_w)^{2/3} B_s = 5.2\ \mu\mathrm{G}\ \left(\frac{n_d}{150}\right)^{2/3} \tag{38}$$

where the estimates of the density at the base of the wind, $\rho_w \simeq 2 \times 10^{-13}$ g cm^{-3} and the field at the surface of the star, $B_s \simeq 4$ G are used. The field expelled by massive stars are unlikely to pervade the volume, and the major contribution would be from supernovae. Although the number of massive stars are of the same order as the number of supernovae using the Salpeter IMF (estimated by

integrating the mass range above 10 $M_\odot$; see the footnote in Sect. 2.2), the smaller fluxes of the wind ($\sim B_{\rm s}R_*^2$ where R_* is the radius of the star) render the effective field strength to be weak. *The key point here, is that for typical values of the halo parameters, $B_{\rm sn}$ is about 10^{-4}–10^{-5} G which is a factor of 10–100 higher than the value in our galaxy ($V_{\rm d} = 6\times10^{11}\,{\rm pc}^3, N\sim 3\times10^8, B_{\rm sn} = 3\ \mu$G) due to a smaller value of $V_{\rm d}/N$ of the supernovae shells.*

4. Accretion to a compact region

Here we consider different viscosity prescriptions, namely direct magnetic stress, the phenomenological α viscosity (Shakura & Sunyaev 1973) derived from magnetic fields, and angular momentum transfer mediated by self-gravity induced instabilities, and calculate the corresponding accretion timescales. The time dependent disk accretion is described by the conservation of mass, radial momentum (where all other forces except gravity are neglected, and $v_{\rm r}/v_\phi \ll 1$) and angular momentum

$$r\partial_{\rm t}\Sigma = -\partial_{\rm r}(r\Sigma\ v_{\rm r}) \tag{39}$$

$$\omega^2 = (1/r)\partial_{\rm r}\Phi \tag{40}$$

$$\Sigma v_{\rm r}\partial_{\rm r}(r^2\omega) = 1/r\ \partial_{\rm r}(r^2\Pi_{{\rm r}\phi}), \tag{41}$$

where $\Sigma(r,t)$ is the surface density, Φ is the gravitational potential and $\Pi_{{\rm r}\phi}$ is the vertically integrated stress. We take r_0 as the inner radius of the disk flow and the outer edge of the compact region while

$$\omega(r) = \frac{\omega_0}{\sqrt{1+(r/r_0)^2}}. \tag{42}$$

By integrating Eq. (41), we obtain for steady flow

$$\dot{M}\omega\left(1-\frac{r_0^2\omega_0}{2r^2\omega}\right) = 2\pi\Pi_{{\rm r}\phi}. \tag{43}$$

The viability of the various alternatives for the viscous stress can be assessed by estimating the accretion rates. In the initial phase of accretion the potential is dominated by the halo as calculated in Sect. 5, while in the later phase, self-gravity dominates and the resulting flow is calculated in Sect. 6.

4.1. Magnetic stress

We consider now the form of the stress tensor that is entirely due to magnetic fields. We assume that the magnetic field injected is largely in the form of small scale loops that are frozen into the plasma. Further, we expect that the processes of compression and advection preserves the form given by

$$B = B_{\rm s}(\rho/\rho_{\rm s})^{2/3} \tag{44}$$

that is likely to be valid for small scale fields in the non-dissipative limit. The Lorentz force on the plasma is

$$(\boldsymbol{J}\times\boldsymbol{B})_\phi = \frac{1}{4\pi}\ \left[\frac{1}{r}\,B_{\rm r}\,\partial_{\rm r}(rB_\phi) + B_z\,\partial_z B_\phi\right], \tag{45}$$

where the first term on the right hand side is the local shear stress and the second term is negligible in the initial phase (the vertical average of small scale fields, $B_z\langle\partial_z B_\phi\rangle \approx 0$), but it could be important during a later phase of accretion where magnetic braking can operate via built up, large scale B_z, by angular momentum transfer to the parts external to the compact region. Here, we take only the local shear stress $\approx B^2H/(2\pi)$ and this was assumed to be initially at sub-equipartition levels as a thermal pressure ($\zeta = 1$) was used for calculating the half-thickness of the initial disk in Eq. (34). One can verify this through a consistency check by using the definition, $\zeta = 1 + B_{\rm sn}^2/(8\pi\rho c_{\rm s}^2)$, which determines the half-thickness, $H\propto\sqrt{\zeta}$ from the condition of vertical equilibrium, (34), $B_{\rm sn}\propto\zeta^{-2/3}$, from Eq. (36), and $\rho\propto\zeta^{-1/2}$ from Eq. (37). It follows that

$$0.03\,\zeta^{-1/6} + 1 = \zeta \tag{46}$$

and for a reasonable choice of parameters ($\nu_{200} = 1, f_* = 0.2, z_{\rm c} = 3.6, \lambda_{\rm v} = 0.075$) this results in $\zeta = 1.03$. Low values of $1/\beta = B_{\rm sn}^2/(8\pi\rho c_{\rm s}^2) \sim 0.03$, are typical for the range of interest in the parameter space.

Next, we estimate the accretion time scale and hence the viability of magnetic accretion in the steady limit. For typical values of the parameters assumed here ($\lambda_{\rm v} = 0.075, \theta = 1/8$) the accretion rate turns out to be

$$\begin{aligned}\dot{M} &= \left|\frac{2\pi\Pi_{{\rm r}\phi}^{\rm m}}{\omega}\right| \sim \frac{B^2H}{\omega} = \left(\frac{H}{r_{\rm d}}\right)\frac{r_{\rm d}^2B^2}{v_{\rm c}}\\ &= 0.2\ B_{-5}^2\ \left(\frac{4.6}{1+z_{\rm c}}\right)^3\ M_\odot\ {\rm yr}^{-1},\end{aligned} \tag{47}$$

using Eqs. (34), (22), (43). Taking the initial field to be from supernovae expulsions ($B = B_{\rm sn}$) from Eq. (36), this implies a time scale of magnetic accretion,

$$\begin{aligned}t_{\rm m} &= 10^8\,M_\odot\,\frac{\mathtt{m}_{\rm h8}}{\dot{M}}\\ &\sim 2\times10^8\ {\rm yrs}\ \frac{4.6}{1+z_{\rm c}}\ \mathcal{M}_{10}^{-2/3}\\ &\quad\times\nu_{200}^{-4/3}\ \left(\frac{0.2}{f_*}\right)^{4/3}\mathtt{m}_{\rm h8}\ \left(\frac{0.1}{f_{\rm b}}\right)^{4/3}.\end{aligned} \tag{48}$$

Having obtained this fast timescale to accrete $10^8\ M_\odot$ of gas, we proceed to calculate the detailed form of $\Pi_{{\rm r}\phi}^{\rm m}$. The thickness of the disk is given by Eq. (34), the balance of the total pressure gradient and vertical gradient of the background potential. Combining Eqs. (34), (44), and $\rho = \Sigma/(2H)$, we obtain

$$\Pi_{{\rm r}\phi}^{\rm m} = -(B_{\rm s}^2/4\pi)\rho_{\rm s}^{-4/3}\Sigma^{4/3}r^{-1/3}\theta_0^{-1/3} \tag{49}$$

where $\theta_0 = 2\theta(\mathcal{M}_{10}/x_{\rm v})^{1/2}$ is the flaring angle of the full thickness of the disk. Initially, the magnetic pressure is lower than the thermal pressure but as the matter sinks into a compact region the magnetic pressure is expected to dominate the vertical pressure gradient.

4.2. α viscosity

If a small scale dynamo operates quickly (Kasantsev 1967; Kulsrud & Anderson 1992) then it will saturate near equipartition values (as is well known from simulations – Hawley et al. 1995 and references therein) and an appropriate form of the stress can be described in terms of a prescription of the form $\Pi^{\rm ss}_{{\rm r}\phi} = -2{\rm H}\alpha_{\rm ss}P$, where $P = \zeta\rho c_{\rm s}^2$ is the total pressure, which is proportional to the gas pressure at equipartition. The accretion time scale is expected to be similar to the one obtained earlier. The dependence on the halo parameters can be expressed in the isothermal limit as

$$t_\alpha \sim 2\times10^8 \text{ yrs } \frac{0.1}{\alpha_{\rm ss}} \left(\frac{4.6}{1+z_{\rm c}}\right)^{1/2} \frac{0.1}{f_{\rm b}} \times \mathcal{M}_{10}^{-2/3} \left(\frac{0.8}{1-f_*}\right) \mathtt{m}_{\rm h8}. \quad (50)$$

Note that, although we use a direct magnetic stress in our calculations, we record for comparison, the detailed form of the α prescription in Appendix B.

4.3. Gravitational instabilities

Cold, thin rotating discs are known to be unstable and the basic stability criteria was provided by Toomre (1964). For a uniformly rotating isothermal disk (Goldreich & Lynden-Bell 1965) the criteria for local stability is given by

$$Q_{\rm T} = \frac{c_{\rm s}\omega}{G\Sigma} \geq 1.06. \quad (51)$$

We find that

$$Q_{\rm T} = \frac{\pi v_{\rm c}^2 H}{GM_{\rm d}} = \frac{\pi}{8}\,\mathcal{M}_{10}^{-1/3} \left(\frac{4.6}{1+z_{\rm c}}\right)^{1/2} \frac{0.8}{1-f_*}\,\frac{0.1}{f_{\rm b}}, \quad (52)$$

where the values ($\theta = 1/8, \lambda_{\rm v} = 0.075$) were assumed. So the disk is unstable to gravitational instabilities and it is possible for angular momentum transport to occur through this process. Lin & Pringle (1987) estimate an effective kinematic viscosity for gravitational instability from $\nu_{\rm e} = \omega\ell^2$, where the critical shearing length, $\ell = G\Sigma\omega^{-2}$ was taken to be the maximum possible size for the instability. Here we make a more conservative estimate by introducing the parameter, $Q_{\rm T}^2 < \alpha_{\rm g} < 1$, into the stress given by

$$\Pi^{\rm g}_{{\rm r}\phi} = \alpha_{\rm g}\,\nu_{\rm e}\,\Sigma\, r\partial_{\rm r}\omega = -\alpha_{\rm g}\,G^2\,\Sigma^3\,\omega^{-2} \quad \text{if} \quad Q_{\rm T} < 1. \quad (53)$$

The corresponding timescale of accretion is

$$t_{\rm g} \sim 10^8\,M_\odot \left|\frac{\omega\,\mathtt{m}_{\rm h8}}{2\pi\,\Pi^{\rm g}_{{\rm r}\phi}}\right| = 10^8{\rm yrs}\mathcal{M}_{10}^{1/2} \times \left(\frac{4.6}{1+z_{\rm c}}\right)^3 \left(\frac{0.8}{1-f_*}\right)^3 \left(\frac{0.1}{f_{\rm b}}\right)^3 \frac{0.1}{\alpha_{\rm g}}\,\mathtt{m}_{\rm h8}. \quad (54)$$

5. Self-similar evolution of the disk in a background potential

Having demonstrated that the time scales of accretion are quite fast, we now proceed to calculate a detailed model of self-similar evolution of a disk from the diffusion equation obtained from the conservation laws (39–41)

$$\partial_{\rm t}\Sigma = \frac{1}{r}\partial_{\rm r}\left(\frac{1}{\partial_{\rm r}(r^2\omega)}\partial_{\rm r}[r^2\Pi_{{\rm r}\phi}]\right), \quad (55)$$

where the viscous stress can be parameterized as $\Pi_{{\rm r}\phi} = -K_2\Sigma^b r^c$ and in addition the rotation law is assumed to be of the form $\omega = K_1 r^a$. This very useful formulation of a self-similar form is due to Pringle (1981) but only particular analytic solutions to the diffusion equation has been reported for the specific cases of ($a = -3/2, b = c = 3$; Lin & Pringle 1987) in the context of accretion of a protostellar disk onto a point mass via gravitational instabilities and ($a = -3/2, b = 5/3, c = -1/2$; Cannizzo et al. 1990 (CLG), see Appendix B of this paper) in the context of disk accretion of a tidally disrupted star onto a massive black hole. Note that in CLG, the scaling law for the viscous stress by the closure of the conditions of local dissipation in an alpha disk in a Kepler potential and vertical equilibrium. Here, an analytic solution to the general problem of the type ($\Pi_{{\rm r}\phi} \propto \Sigma^b r^c, \omega \propto r^a$) is presented so that possible viscosity mechanisms discussed earlier and expressible in this way, can be explored within the same formulation. In the magnetic case given below, the viscosity scaling is due a magnetic stress, the flux-freezing condition and vertical equilibrium in a cold disk in the background halo potential. A solution for an alpha disk with local dissipation with a general rotation law is provided in Appendix B. The general solution presented below has a larger utility in contexts other than one considered here.

If $b = 1$, the equation is linear and the general solution is easily found. Proceeding generally, under the assumptions of self-similarity for ($b \neq 1$), one may write the the surface density in the following form

$$\Sigma = \Sigma_0(t/t_0)^\beta g(\xi) \quad r_{\rm f} = r_{\rm s}(t/t_0)^\alpha, \quad (56)$$

where $\xi \equiv r/r_{\rm f}$, and $r_{\rm s}$ is the associated radius scale. We set the constants

$$t_0 = \frac{K_1}{K_2} r_{\rm s}^{a+2-c}\Sigma_0,\ M_{\rm d} = 2\pi l\Sigma_0 r_{\rm s}^2,\ l = \int_0^1 \xi^2 g(\xi){\rm d}\xi \quad (57)$$

where $M_{\rm d}$ is the initial disk mass. Here we seek a particular solution when there is no external torque, which implies the total angular momentum, J, of the disk is a constant. Using the scaling relations above that are implicit in Eq. (55) and

$$J = 2\pi K_1 r_{\rm s}^{4+a}\Sigma_0 j, \qquad j = \int_0^1 \xi^3 g(\xi){\rm d}\xi \quad (58)$$

it follows that $\alpha = (4b + ab - 2 - c)^{-1}$ and $\beta = -(a+4)\alpha$. At this point we note that the disk edge travels outward if $2 + c < b(4 + a)$. Substituting into the form for the surface

density, as given in (56), and simplifying (55), we obtain the following ordinary differential equation,

$$-\alpha\xi g' + \beta g = -\frac{1}{(a+2)\xi}\mathrm{d}_\xi\left(\xi^{-(a+1)}\mathrm{d}_\xi(\xi^{2+c}g^b)\right). \quad (59)$$

After some algebraic transformations, one can integrate it once to obtain

$$\alpha(a+2)g\xi^{a+4} + (a-c)\xi^{2+c}g^b = b\xi^{3+c}g^{b-1}g' + c_1. \quad (60)$$

Now, we apply the boundary condition that the density vanishes at the disk edge, ie.,

$$\Sigma(r = r_\mathrm{f}) = 0; \quad g(1) = 0. \quad (61)$$

Moreover, if $b > 1$, which is the case for the examples considered here, then $c_1 = 0$. By rearranging terms and integrating, we obtain the following solution

$$g(\xi) = \xi^{(a-c)/b}\left(1 - \xi^{2+\frac{(a-c)}{b}}\right)^{1/(b-1)}. \quad (62)$$

The time constant can be evaluated with $r_\mathrm{s} = r_\mathrm{d}$ to be

$$t_0 = \frac{\omega}{|\Pi_{\mathrm{r}\phi}(\Sigma_0, r_\mathrm{d})|}\frac{M_\mathrm{d}}{2\pi l} = t_\mathrm{a} l^{b-1}\ \frac{M_\mathrm{d8}}{\mathtt{m}_\mathrm{h8}}, \quad (63)$$

where t_a is the accretion time scale calculated in Sect. 4.1 and Sect. 4.3 in the steady case using $\Pi_{r\phi}(M_\mathrm{d}/(2\pi r_\mathrm{d}^2), r_\mathrm{d})$. The rate at which mass sinks into the center is given by

$$M_\mathrm{c}(t) = M_\mathrm{d}\left[1 - \left(\frac{t}{t_0}\right)^{-(a+2)\alpha}\right]. \quad (64)$$

The accretion time scale which is the time that transpires when a fraction $\epsilon = \mathtt{m}_\mathrm{h8}/M_\mathrm{d8}$ of the disk mass falls in is given by

$$\begin{aligned}\tau_\mathrm{a} &= t_0\ \left((1-\epsilon)^{\frac{-1}{(a+2)\alpha}} - 1\right)\\ &= t_\mathrm{a}\ l^{b-1}\ \left((1-\epsilon)^{\frac{-1}{(a+2)\alpha}} - 1\right)\ \epsilon^{-1}\end{aligned} \quad (65)$$

where t_a represents the timescales $t_\mathrm{m}, t_\mathrm{g}$ or t_α, and indicates that the estimates derived earlier are modified by geometric factors. Now we consider the particular case of magnetic accretion ($a = -1, b = 4/3, c = -1/3, \epsilon = 1/8$, see Sect. 4.1 where the value of ϵ is chosen for a typical case where the disk mass, $M_\mathrm{d8} = 8$, and $\mathtt{m}_\mathrm{h8} = 1$) which has the solution

$$\begin{aligned}\alpha = 3/7, \quad \beta = -9/7,\ \tau_\mathrm{m} = 1.01\, t_\mathrm{m},\\ g_\mathrm{m}(\xi) = \xi^{-1/2}\left[1 - \xi^{3/2}\right]^3.\end{aligned} \quad (66)$$

Similarly, the accretion due to gravitational instabilities ($a = -1, b = 3, c = 2, \epsilon = 1/8$, $M_\mathrm{d8} = 8$, and $\mathtt{m}_\mathrm{h8} = 1$, see Sect. 4.3) has the solution

$$\begin{aligned}\alpha = 1/5, \quad \beta = -3/5,\ \tau_\mathrm{g} = 0.54\, t_\mathrm{g},\\ g_\mathrm{g}(\xi) = \xi^{-1}\left[1 - \xi\right]^{1/2}.\end{aligned} \quad (67)$$

The disk structure of these solutions are shown in Fig. 5. The self-similar solutions of this kind to (55) are known to develop at large times in numerical simulations with a variety of initial conditions (Lin & Pringle 1981).

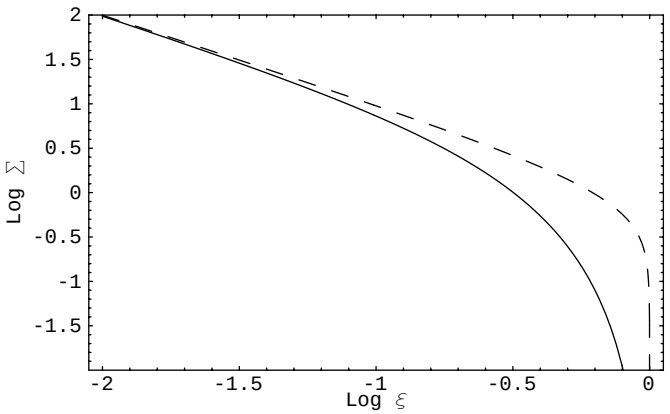

Fig. 5. The structure $g(\xi)$ of the self-similar disk, $\Sigma = \Sigma_0\left(\frac{t}{t_0}\right)^\beta g(\xi)$ where $\xi = r/r_\mathrm{f}, r_\mathrm{f} = r_\mathrm{s}\left(\frac{t}{t_0}\right)^\alpha$. The magnetic solution, $g_\mathrm{m}(\xi) = \xi^{-1/2}\left[1 - \xi^{3/2}\right]^3$ is shown by a solid-line, and the solution of the disk with gravitational viscosity, $g_\mathrm{g}(\xi) = \xi^{-1}\left[1 - \xi\right]^{1/2}$, is shown by a dashed line.

Now we determine the regime in parameter space where the halo dominated flow can occur. This is given by the condition that at $t = t_0$ and $r = r_\mathrm{d}$, the halo dominates self-gravity or

$$\begin{aligned}\frac{v_\mathrm{c}^2}{r_\mathrm{d}} &> \left.\frac{\mathrm{d}\Phi_\mathrm{d}}{\mathrm{d}r}\right|_{r=r_\mathrm{d}}\\ \frac{M_\mathrm{h}}{r_\mathrm{d} r_\mathrm{v}} &> \frac{M_\mathrm{d}}{l r_\mathrm{d}^2}\ \sum_n \alpha_n^2 J_1(\alpha_n)\ \int_0^1 J_0(\xi\alpha_n) g(\xi)\xi\mathrm{d}\xi,\end{aligned} \quad (68)$$

where v_c is the circular velocity due to the halo alone, the disk potential was expressed as a Bessel transform of the surface density and α_n are the zeros of J_0. The collapse factor $r_\mathrm{v}/r_\mathrm{d} = s\sqrt{k_1}/\lambda_\mathrm{v} = (j/l)\sqrt{k_1}/\lambda_\mathrm{v}$ from Sect. 2.1, $M_\mathrm{h}/M_\mathrm{d} = (1 - f_\mathrm{g})/f_\mathrm{g}$ by definition, leading to

$$\frac{\lambda_\mathrm{v}(1-f_\mathrm{g})}{f_\mathrm{g}\sqrt{k_1}} > \frac{j}{l^2}\sum_n \alpha_n^2 J_1(\alpha_n)\ \int_0^1 J_0(\xi\alpha_n) g(\xi)\xi\mathrm{d}\xi. \quad (69)$$

For the solution (66), the magnetic case, the RHS of the above equation works out to be 0.44 and for the gravitational instability case, the solution (67), the corresponding value is 0.46. Hence this condition can be written as

$$\frac{\lambda_\mathrm{v}(1-f_\mathrm{g})}{f_\mathrm{g}} > 0.32 \quad (70)$$

where $k_1 = 0.5$ for a truncated isothermal sphere was used. For a reasonable range in the parameters ($\lambda_\mathrm{v} = 0.05$–$0.1$, $f_\mathrm{g} = 0.05$–0.08) the above condition holds good ($\lambda_\mathrm{v}(1 - f_\mathrm{g})/f_\mathrm{g}$ is in the range 1–4); as a result, the initial accretion flow is expected to be halo dominated. As the mass accretes into the center, the spin deviates from $\omega \propto 1/r$ and gradually increases. The self-similar solutions are valid only up to a point beyond which the self-gravity due the disk and the central mass dominates the potential.

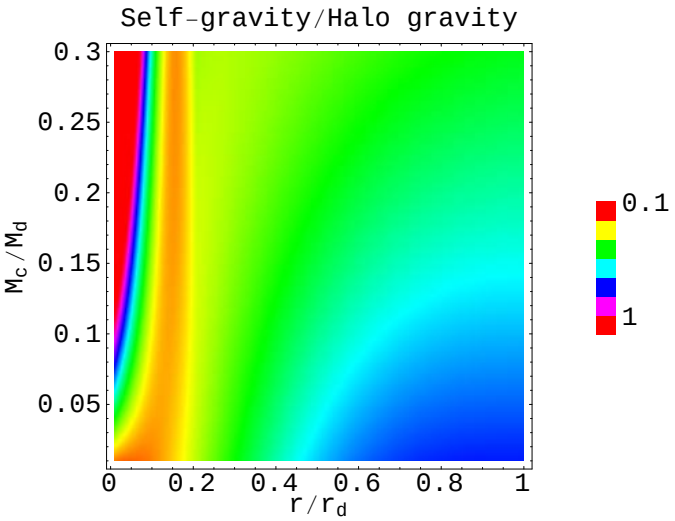

Fig. 6. A density plot of the ratio of self-gravity (disk and the central mass) to halo gravity defined as $\frac{1}{v_c^2}\left(r\frac{\mathrm{d}\Phi_\mathrm{d}(r,t)}{\mathrm{d}r}+\frac{GM_\mathrm{c}(t)}{r}\right)$, showing the evolution of a magnetized disk in the halo potential as the central mass increases to $\epsilon = M_\mathrm{c}/M_\mathrm{d} = 0.3$. The horizontal axis is the in units of the initial disk radius, r_d. The value of $\lambda_\mathrm{v}(1-f_\mathrm{g})/(f_\mathrm{g}\sqrt{k_1})$ was chosen to be 3; the halo gravity (in units of v_c^2) dominates at radii outside a central region of $y \sim 0.1$. This figure can be seen in color in the online version of the journal.

The time of transition to a self-gravitating flow can be estimated by seeking that

$$r\frac{\mathrm{d}\Phi_\mathrm{d}(r,t)}{\mathrm{d}r}+\frac{GM_\mathrm{c}(t)}{r} > v_\mathrm{c}^2. \tag{71}$$

Now expressing time in terms of the $\epsilon = M_\mathrm{c}/M_\mathrm{d}$ in Eq. (64), we obtain after some algebra

$$(1-\epsilon)^3\frac{jy}{l^2}\left[\sum_n \alpha_n^2 J_1(\alpha_n(1-\epsilon)y)\int_0^1 J_0(\xi\alpha_n)g(\xi)\xi\mathrm{d}\xi\right] + \frac{\epsilon j}{ly(1-\epsilon)} > \frac{\lambda_\mathrm{v}(1-f_\mathrm{g})}{f_\mathrm{g}\sqrt{k_1}}, \tag{72}$$

where $y = r/r_\mathrm{d}$. Clearly, this condition does not hold close to a compact central region (defined by $r < r_0$) where it is dominated by the central mass. The solutions considered here are a good approximation for the region beyond $y = 0.1$ for $\epsilon < 0.3$ and provide a sufficiently accurate description (See Fig. 6). At large times, a Keplerian flow into the compact region can be assumed to occur and one can use a self-similar flow again with $a = -3/2$ and the corresponding magnetic stress taking into account $v_\mathrm{c} \propto r^{a+1}$ in Eq. (34) (in combination with (44), and $\rho = \Sigma/(2H)$) leads to $\Pi^\mathrm{m}_{\mathrm{r}\phi} \propto \Sigma^{4/3}r^{a/3} = \Sigma^{4/3}r^{-1/2}$. Similarly $\Pi^\mathrm{g}_{\mathrm{r}\phi} \propto \Sigma^3 r^{-2a} = \Sigma^3 r^3$ from Eq. (53). However, the estimate of the accretion timescale is not expected to be very different from the one derived earlier. The key result is that about a fraction, 0.3, of the disk mass can be transported into a central region, which is a fraction, $y = 0.1$, of the initial disk radius within the time given by the solutions (66). For typical values, this implies that about $2\times10^8\ M_\odot$ of gas sinks into a $r_0 = 0.1r_\mathrm{d} \sim 100$ pc region in a halo (with $\mathcal{M}_{10} = 1, \lambda_\mathrm{v} = 0.075$) in a timescale of 2×10^8 yrs.

6. Disk evolution in a self-gravitating regime

We now examine the evolution of the disk in a gravity field that is entirely due to itself. This flow can occur after sufficient accretion of mass into a compact region of radius r_0; or, alternatively at the time of the formation of the disk if the Eq. (70) is not satisfied and $\lambda_\mathrm{v}(1-f_\mathrm{g})/f_\mathrm{g} \lesssim 0.32$. The problem of self-gravitating accretion flow is complicated by the coupling of Poisson's equation to the momentum and continuity equations. Clearly, its evolution has to be treated differently from the preceding case of a prescribed background potential. A detailed model is deferred to a work in preparation (Mangalam 2001); below, we consider a useful simplified version of the problem by assuming a particular form of the density distribution (see Field 1994).

We assume a Mestel (1963) disk where the self-consistent density distribution with potential is entirely due to self-gravity, is of the form

$$\Sigma(r,t) = \frac{v_\phi^2(t)}{2\pi G r}, \tag{73}$$

where the time dependence appears only in the rotational velocity. This is a an interesting disk which is self-consistent, taking into account the most relevant physics. Taking

$$v_\phi = v_0\,\chi(t) \quad \text{and} \quad r = r_0\,\chi_1(t)\,x \tag{74}$$

where $v_0^2 = GM_\mathrm{c}/r_0$, and M_c is the mass out to r_0. We see that by assuming a self-similar evolution of the disk, the mass out to a given x should be independent of t and hence it follows that

$$\chi_1 = \chi^{-2} \quad \text{and} \quad \Sigma = \Sigma_\mathrm{c}\,\frac{\chi^4}{x}, \tag{75}$$

where $\Sigma_\mathrm{c} = M_\mathrm{c}/(2\pi r_0^2)$. From the continuity equation,

$$r\partial_\mathrm{t}\Sigma + \partial_\mathrm{r}(r\Sigma v_\mathrm{r}) = 0 \tag{76}$$

we find

$$v_\mathrm{r} = -4\chi^{-3}\dot{\chi}r_0 x. \tag{77}$$

Substituting this and the self-similar forms given above into the angular momentum equation,

$$\begin{aligned}\Sigma\partial_\mathrm{t}v_\phi + \Sigma(v_\mathrm{r}/r)\partial_\mathrm{r}(rv_\phi) &= (1/r^2)\partial_\mathrm{r}(r^2\Pi_{\mathrm{r}\phi}) \\ -3v_0\Sigma_\mathrm{c}\chi^2\dot{\chi} &= \frac{1}{x}\frac{\mathrm{d}}{\mathrm{d}x}\left(x^2\Pi_{\mathrm{r}\phi}\right),\end{aligned} \tag{78}$$

we obtain

$$\Pi_{\mathrm{r}\phi} = -\frac{3}{2}v_0\Sigma_\mathrm{c}r_0\chi^2\dot{\chi}, \tag{79}$$

which is *independent* of x. So far no specific viscosity mechanism has been invoked – the form of $\Pi_{\mathrm{r}\phi}$ above is necessitated by the prescription of a Mestel disk. If a magnetic

stress is assumed and $\Pi_{r\phi} = -\kappa B^2 H/(2\pi)$, where κ is a factor of order unity and B is given by the vertical balance of magnetic pressure and gravity, $B = 2\pi\sqrt{G\Sigma} = 2\pi\sqrt{G\Sigma_c}\chi^4/x$. It follows that the half thickness, $H \propto x^2$, and can be expressed as $H = H_0 x^2 \chi^p$. Furthermore, from the flux-freezing condition, $B \propto \left[r^2 H\right]_{x=1}^{2/3}$, it is seen that $p = -2$. Equating the form of $\Pi_{r\phi}$ from Eq. (79) to a magnetic stress, $\kappa B^2 H/(2\pi)$, and writing (after taking $\theta = 1/8, \lambda_v = 0.075$)

$$\tau = \frac{1}{2}\frac{v_0 r_0^3}{GM_c H} = \frac{r_0}{v_0}\,\frac{1}{2\kappa}\,\frac{r_0}{H_0} \sim 10^6 \left(\frac{r_0/r_d}{0.1}\right) \mathcal{M}_{10}^{1/3}\,\frac{4.8}{1+z_c}\ \text{yrs}, \quad (80)$$

we see that

$$3\tau\,\chi^2\,\dot{\chi} = \chi^6, \quad (81)$$

which leads to the solution

$$\chi(t) = \left(\frac{\tau}{\tau - t}\right)^{1/3}, \quad (82)$$

where $\chi(0) = 1$ was taken as the initial condition. So the disk spins up rapidly and shrinks to a smaller radius. Clearly, the solution is no longer valid when it is relativistic. The self-similar collapse of the compact region is only a sketch but nevertheless the collapse timescale, τ, suggests that formation of a black hole is extremely rapid ($\sim 10^6$ yrs).

7. Summary of the results and discussion

We summarize our results as follows:

1. We considered star formation and supernovae feedback on the remaining gas in the halo based on the framework of DS. We include a new and necessary condition C2, namely that escape time for the hot gas be shorter than the cooling time and find that the condition for gas loss can be expressed by Eqs. (27), (23), (29) which is depicted in Fig. 3. For a typical choice of f_* and ν, Fig. 4 shows the allowed range for Halo mass in terms of redshift. There is a sharp decline in the allowed range beyond collapse redshifts of $z_c = 2$, as the potential wells formed at earlier epochs are deeper and trap the gas better.
2. It was seen in Sect. 2.3 that the hot gas from supernovae has a filling factor of nearly unity and hence the small-scale magnetic fields occupy the disk. It was shown in Sect. 3 the field strength is significant (10–100 μG), based on typical values of supernova efficiency, ν, and star fraction, f_*.
3. In Sect. 4, we examined magnetic stress and viscosity due to self-gravity induced instabilities that would operate in a collapsed disk. The accretion timescales were estimated for a direct magnetic stress, Eq. (48), an α prescription, Eq. (50), and self-gravity, Eq. (54), in terms of halo parameters $(\mathcal{M}, z_c)$ and star formation parameters (f_*, ν). The timescales are all short compared to the cosmic time.
4. A general solution for a self-similar and time dependent accretion flow for a viscous stress of the form $\Pi_{r\phi} \propto \Sigma^b r^c$ in a prescribed potential, $\omega \propto r^a$, was obtained in Sect. 5. This was applied to the specific cases of magnetic accretion, Eq. (66) and and gravitational instabilities, Eq. (67). The structure of the resulting disk is shown in Fig. 5 and the timescales are within geometric factors of their estimates. The disk eventually becomes fully Keplerian. The condition of halo dominated flow is given by Eq. (70) and the transition to a self-gravitating flow is given by Eq. (72). This solution is valid for dominant halos in the initial stages for the outer parts, $y > 0.1$, oustide a Keplerian compact region for up to time when a fraction of the disk mass, $\epsilon \sim 0.3$, falls in (see Fig. 6).
5. A self-gravitating Mestel disk that is spinning up as it is collapsing self-similarly, is described in Sect. 6. We apply this to a compact region where the pressure is assumed to be due to magnetic fields. The time scale of collapse turns out to be the rotation time of the outer radius, which is a few million years.

We now discuss some of the issues involved:

Supernovae feedback

In a pioneering work, DS, showed that with a model of protogalactic gas in a halo reproduces the observed relations very well with an initial CDM model. Further, the condition for gas loss was given by the condition that the energy input from supernovae is more than the binding energy, C1 and the cooling condition for gas contraction and star formation. In this work, we specify an additional necessary condition, C2, that the escape time be shorter than the cooling time. As indicated in Fig. 3, this restricts the gas loss to the halos in the shaded region. The exact shape and location of the region is subject to the choice of parameters (ν, f_*), but the key point made here is that the entire region to the left of C1 cannot be considered as a gas loss zone, even if heating by background UV photons were included. It is worth investigating this question in more detail by simulations that include the hydrodynamics and cooling of the hot gas. Based on this study, one can conclude that most of the dwarf galaxies involved efficient conversion of stars or high efficiency of supernovae, since that would place curve C2, higher on the cooling diagram accounting for the prediction of the location of the dwarf galaxies made by DS. The constraints imposed here, however, account for the presence of black hole systems on the left of C1 (and above C2). It also explains a sharp decline in quasars at epochs later than $z = 2$.

Magnetic field strength in supernovae shells

In estimating the field strength B_{sn} in Sect. 3, all the shells were assumed to have 10^{-4} G when they are young (size of 0.8 pc) and flux freezing was used to estimate the

values at a given size. This field has been measured in the Crab nebula and in other young supernova remnants like Tycho, Kepler and Cas A, the field strength in the shell is inferred to be 10^{-3}–10^{-4} G (Strom & Duin 1973; Henbest 1980; Anderson et al. 1991). Simulations by Jun & Norman (1996), show local turbulent amplification by Rayleigh-Taylor and Helmholtz instabilities but claim overall sub-equipartition strengths. An analysis of Cas A X-ray and radio surface brightness at high resolution, show that there is a strong correlation, implying a possible equipartition between the field (∼mG) and the hot gas (Keohane et al. 1998). The field amplification can be from other sources as well. For example, the magnetic field in the Crab has been wound up in the body of the nebula by the pulsar and the magnetic energy is a few a percent of the spin energy (Rees & Gunn 1974). High resolution simulations of a supernova including rotation and expanding in an unmagnetized medium, which to our knowledge are unavailable, are best suited to the answer the question of the initial field strength in the disk. The small scale fields that are injected in the medium could be amplified to saturation levels by a dynamo operating in the disk aided by differential rotation and turbulent motion. Since this amplification was not taken into account (no assumption other than flux-freezing was made for the field evolution), the field strengths derived from supernovae which is in the range 10–100 μG, could be an underestimate.

Large scale fields

Strong fields of a few μG are estimated from Faraday rotation of background QSOs by damped Lyα absorptions systems, which are thought to be proto-galactic disks, as early as $z \sim 2$, imposing constraints on the kinematic dynamo (Kronberg et al. 1992). A primordial origin for the large scale field in galaxies has been speculated upon (Rees 1994; Ratra 1992 and references therein), but the field generated by these mechanisms is much smaller than the magnitude required for a primeveal hypothesis. Large-scale magnetic fields in the galaxy are thought to be generated by a turbulent dynamo from a weak seed field ($\sim 10^{-19}$ G). But, it has been argued that magnetic energy at small (eddy) scales builds up much faster (at eddy turnover rates) than the mean field, so that the kinematic dynamo shuts off before the large scale fields amplify to observed levels (Kulsrud & Anderson 1992; Kasantsev 1967) if the initial seed is weaker than 10^{-9} G. Subramanian (1998) argues, however, that the fields are intermittent and do not fill the volume. The small scale flux ropes are at saturated values but the mean energy density is at sub-equipartition levels allowing the large scale field to grow to equipartition strength, aided by ambipolar drift. This question is still unresolved, but if the supernovae field can provide a fairly strong seed field ($\gtrsim 10^{-9}$ G), then a kinematic dynamo can operate to amplify the fields to μG strengths in a galactic disk. A sphere of radius L, encloses $(L/r_{\rm sn})^3$ remnants where $r_{\rm sn}$ is the size of a remnant. The rms value of the field at a scale $L > r_{\rm sn}$ would be roughly $\sim B_{\rm sn}(r_{\rm sn}/L)^{3/2}$. At the scale of the compact region, $L = r_0 = 100$ pc, the large scale seed field is of order 10^{-7} G.

Angular momentum transport

There is an angular momentum transport mechanism required to form a seed mass in a central region and one for the compact central mass to further collapse; the two schemes, in principle, can be different. Loeb & Rasio (1994) concluded from hydrodynamic simulations that fragmentation occurs halting a direct collapse to relativistic scales and suggested that low spin systems could form supermassive seeds of disk or star geometry which would contract under radiative viscosity. The picture proposed here is that direct magnetic stress or gravitational instabilities in the disk can transport matter into a compact region on a dynamical timescale. The scheme of gravitational instabilities hinges on $Q_{\rm T} < 1$ in the disk whereas the direct magnetic stress depends on the supernova efficiency and field expulsion. The presence of high magnetic energy density from MHD turbulence has been invoked to explain high velocity dispersions of H I clouds in galactic disks (Sellwood & Balbus 1999).

Angular momentum in the inner region ($\lesssim$1 pc) is likely to be more complicated due to radiation pressure that would prevent collapse. The model of self-gravitating magnetized collapse in Sect. 6 was illustrative of the timescale involved but a detailed model for the inner region that takes into account radiation pressure, radiative viscosity and evolution of the field is required. If dynamo action takes place within the compact region ($\lesssim$100 pc), the exponentiation timescale in the linear regime will be of order $1/\omega(r_0) \sim 10^6$ yrs. The residual large scale seed field ($\sim 10^{-7}$ G) from supernovae can be amplified to dynamical values (mG) in 10^7 years and the e-folding timescale for magnetic braking is $r_0/v_{\rm A} \sim (M(r_0)/r_0)^{1/2}/B = 10^6$ yrs corresponding to this field strength.

8. Conclusions

In this work, a semi-analytic model of quasar formation was attempted which captures the essential details of star formation with supernovae feedback and angular momentum transport via magnetic fields and self-gravity. Based on the results in this work (as summarized in Sect. 7), and for the relevant range in parameter space, it is seen that a 10^{10} $M_\odot$ cloud at z of 8 can collapse to form a gaseous disk in the dark halo by z of 4.8 and about 10^7–10^8 $M_\odot$ of gas (which is 0.01–0.1 of the total disk mass) accretes into a $r_0 \lesssim 100$ pc region in a fast timescale of 10^8 yrs. The magnetic stress from supernovae can be significant in the disk and is preferred over other possibilities as observational evidence exists for star formation, and large scale fields at $z \sim 2$. The collapse solutions do not hinge on the source of magnetic fields- SN or small scale dynamo. The small scale dynamo needs a few rotation time

scales to build up and that could be significant – 10^8 yrs. The arguments for SN fields are given in section Sect. 4.1; the strong fields suggested can cause fast accretion rates instantly after the disk forms. The field strength estimation relies only on flux freezing arguments. Further, the alternative collapse solution using gravitational instabilty is also given.

The solution to the non-linear diffusion equation presented in Sect. 5 can be applied in other contexts, e.g. protostellar disks. As a part of future work it is planned to investigate a detailed model of the inner region using a simulational approach, the impact of the restriction on the mass range of black hole hosts ($\mathcal{M}-z$) by supernovae feedback on the details of the quasar luminosity function, dwarf galaxy formation, and the strength of the large scale seed field.

Acknowledgements. I thank K. Subramanian for discussions. I thank the referee for helpful comments and suggestions.

Appendix A: Core condensation in halos

Here we calculate the change in gravitational potential energy from a truncated isothermal halo to a truncated isothermal halo of stars and dark matter containing an exponential gas disk. The final halo mass, $M_{\rm h} = (1 - f_{\rm g})\mathcal{M}$ is taken to be due to stars and dark matter, and remaining mass is in the form of a gaseous disk with $M_{\rm d} = \mathcal{M} f_{\rm b}(1 - f_*) = f_{\rm g}\mathcal{M}$ where $f_{\rm g}$ is the gas fraction. The initial potential energy is given by

$$W_{\rm i} = -\frac{G\ \mathcal{M}^2}{2r_{\rm v}}\cdot \tag{A.1}$$

The final potential energy is given by

$$W_{\rm f} = -\frac{GM_{\rm h}^2}{2r_{\rm v}} - 0.3\frac{GM_{\rm d}^2}{r_{\rm d}} + \frac{1}{2}\int(\rho_{\rm d}\Phi_{\rm h} + \rho_{\rm h}\Phi_{\rm d})\,{\rm d}V, \tag{A.2}$$

where the first two term represents the self potential energies due a truncated isothermal halo of size $r_{\rm v}$, and an exponential disk of size $r_{\rm d}$, respectively, and the third term is due to the interaction between them. The first part of the last term with (the disk surface density $\Sigma(r) = \exp(-r/r_{\rm d})\ M_{\rm d}/(2\pi r_{\rm d}^2)$ and $\Phi_{\rm h} = GM_{\rm h}/r_{\rm v}$)can be reduced to $-(1/2)(GM_{\rm d}M_{\rm h}/r_{\rm v})(1+\exp(-1/\lambda_{\rm v})/\lambda_{\rm v})$ where the term involving $\lambda_{\rm v}$ is negligible in the range of interest for which $0.1 > \lambda_{\rm v} > 0.05$. The second part of the interaction term can be evaluated with the disk potential expressed as a Bessel series in the region $r < r_{\rm v}$ where $\rho_{\rm h} = M_{\rm h}/(4\pi r_{\rm v} r^2)$ contributes. This term works out to be $-(GM_{\rm d}M_{\rm h}/r_{\rm v})0.3/\lambda_{\rm v}$ to a good approximation, where the collapse factor, $r_{\rm v}/r_{\rm d} \simeq 1/\lambda_{\rm v}$, is in the range 10–20 (see Sect. 2.1). Combining the two we obtain

$$\frac{1}{2}\int(\rho_{\rm d}\Phi_{\rm h} + \rho_{\rm h}\Phi_{\rm d})\,{\rm d}V \approx -\frac{GM_{\rm d}M_{\rm h}}{2\ r_{\rm v}}\left(1+\frac{0.6}{\lambda_{\rm v}}\right)\cdot$$

Finally, we obtain the change in gravitational potential energy

$$\Delta W(\mathcal{M}, f_{\rm g}, \lambda_{\rm v}, r_{\rm v}) = \frac{G\mathcal{M}^2}{2\ r_{\rm v}}$$
$$\times\left\{(1-f_{\rm g})^2 - 1 + f_{\rm g}^2\,\frac{0.3}{\lambda_{\rm v}} + f_{\rm g}(1-f_{\rm g})\left(1+\frac{0.6}{\lambda_{\rm v}}\right)\right\}$$
$$= \frac{G\mathcal{M}^2}{2\ r_{\rm v}} f_{\rm g}\left[(2-f_{\rm g})\frac{0.3}{\lambda_{\rm v}} - 1\right] \approx \frac{G\mathcal{M}^2}{r_{\rm v}} f_{\rm g}\left(\frac{0.3}{\lambda_{\rm v}} - \frac{1}{2}\right) \tag{A.3}$$

which is bounded by $0.5\ G\mathcal{M}^2/r_{\rm v}$.

Appendix B: Time-dependent evolution of an alpha disk

Here we first consider a simple polytrope and then discuss the case of a disk coupled with an local energy dissipation condition. By assuming that the gas is a polytrope of index γ,

$$P = K\ (\Sigma/2H)^{\gamma}, \tag{B.1}$$

and using the vertical equilibrium, Eq. (33), we obtain

$$\begin{aligned}\Pi_{{\rm r}\phi}^{\rm ss} &= -2\alpha_{\rm ss}PH \\ &= -\alpha_{\rm ss}K^{2/(\gamma+1)}\Sigma^{(3\gamma+1)/(\gamma+1)}\omega^{2(\gamma-1)/(\gamma+1)}.\end{aligned} \tag{B.2}$$

In some applications it is appropriate to consider a disk with an energy dissipation condition as has been done by Cannizzo et al. 1990 (CLG), for the case of disk accretion of a tidally distrupted star onto a massive black hole. Using the solution presented in Sect. 5, we can generalize to a case of a rotational law, $\omega \propto r^a$, and viscous stress, $\Pi_{{\rm r}\phi} \propto \Sigma^b r^c$. The viscous stress is given by

$$\Pi_{{\rm r}\phi} = -2\alpha_{\rm ss}PH = -\frac{\alpha_{\rm ss}k_{\rm B}T}{\mu{\rm m_p}}\Sigma \tag{B.3}$$

where T refers to the central temperature and P is the gas pressure. Further, in the general prescription, the radiative flux is matched to the viscous dissipation by

$$\alpha_{\rm ss}\omega HP|a| = \frac{4}{3}\ \frac{4\sigma T^4}{\kappa\rho H} \tag{B.4}$$

where σ is the Stefan-Boltzmann constant and $\kappa(\rho, T)$ is the opacity. This reduces to

$$T^3 = \frac{3}{16}\left(\frac{\alpha_{\rm ss}k_{\rm b}}{\mu{\rm m_p}}\right)\omega\Sigma^2\frac{\kappa}{4\sigma}|a|. \tag{B.5}$$

Now, putting this back in Eq. (B.3), we obtain

$$\begin{aligned}\Pi_{{\rm r}\phi} &= -\left(\frac{3}{16}\right)^{1/3}\left(\frac{\alpha_{\rm ss}k_{\rm b}}{\mu{\rm m_p}}\right)^{4/3} \\ &\quad\times\omega^{1/3}\Sigma^{5/3}\left(\frac{\kappa}{4\sigma}\right)^{1/3}|a|^{1/3}.\end{aligned} \tag{B.6}$$

This implies $b = 5/3, c = a/3$ for a constant κ. For the case of a Kepler potential we obtain the scaling (and opacity

due to electron scattering which is a constant) used in CLG ($a = -3/2, c = -1/2, b = 5/3$) and their solution is given by Eq. (62) for these indices. The case of a flat rotation law and opacity due to electron scattering yields ($a = -1, b = 5/3, c = -1/3$). This solution can be easily extended to more general opacities of the form $\kappa \propto \rho^{\mathrm{p}} T^{\mathrm{q}}$, such as the Kramer's, and the appropriate solutions can be easily found.

References

Anderson, M., Rudnick, L., Leppick, P., & Braun, R. 1991, ApJ, 373, 146
Bahcall, J. N., & Soniera, R. M. 1980, ApJS, 44, 73
Barnes, J., & Efsthasiou, G. 1987, ApJ, 319, 575
Binney, J., & Tremaine, S. 1987, Galactic Dynamics (Princeton: Princeton University Press)
Bisnovatyi-Kogan, G. S., Ruzmaikin, A. A., & Sunyaev, R. A. 1973, SvA, 17, 137
Blandford, R. D., & Rees, M. J. 1992, in Testing the AGN Paradigm, ed. S. S. Holt, S. G. Neff, & C. M. Urry (New York: Am. Inst. Phys.), 3
Cannizzo, J. K., Lee, H. M., & Goodman, J. 1990, ApJ, 351, 38 (CLG)
Chevalier, R. A. 1974, ApJ, 188, 501
Dekel, A., & Silk, J. 1986, ApJ, 303, 39 (DS)
Eisenstien, D. J., & Loeb, A. 1995, 443, 11
Ferrara, A., & Tolstoy, E. 2000, 313, 291
Ferrarese, L., & Merritt, D. 2000, ApJ, 539, L9
Field, G. B. 1994, in Cosmical Magnetism, ed. D. Lynden-Bell (Cambridge: Institute of Astronomy, Cambridge)
Ford, H. C., Harns, R. J., Tsvetarov, Z. I., et al. 1994, ApJ, 435, L27
Gebhardt, K., Kormendy, J., Ho, L. C., et al. 2000, ApJ, 543, L5
Goldreich, P., & Lynden-Bell, D. 1965, MNRAS, 130, 125
Haenelt, M. G., & Rees, M. J. 1993, MNRAS, 263, 168
Hamann, F., & Ferland, G. 1992, ApJ, 391, L53
Hawley, J. F., Gammie, C. F., & Balbus, S. A. 1995, ApJ, 440, 742
Heavens, A. F., & Peacock, J. A. 1988, MNRAS, 232, 339
Henbest, S. N. 1980, MNRAS, 190, 833
Jun, B.-I., & Norman, M. L. 1996, ApJ, 465, 800
Kasantsev, A. P. 1968, Sov. Phys. – JETP, 26, 1031
Keohane, J. W., Gotthelf, E. V., & Petre, R. 1998, ApJ, 503, L175
Kormendy, J., & Richstone, D. O. 1995, A&AR, 33, 581
Kronberg, P. P., Perry, J. J., & Zukowski, E. L. H. 1992, ApJ, 387, 528
Kulsrud, R., & Anderson, S. W. 1992, ApJ, 396, 606
Larson, R. B. 1974, MNRAS, 169, 229
Lin, D. N. C., & Pringle, J. E. 1987, MNRAS, 607
Loeb, A., & Rasio, F. A. 1994, ApJ, 432, 52
MacLow, M.-M., & Ferrara, A. 1999, 513, 142
Mangalam, A. 2001, A&A, in preparation
Mestel, L. 1963, MNRAS, 126, 553
Miyoshi, M., Morar, J., Hermsteir, J., et al. 1995, Nature, 373, 127
Natarajan, P. 1999, ApJ, 512, L105
Padmanabhan, T., & Subramanian, K. 1992, BASI, 20, 1
Padmanabhan, T. 1993, Structure Formation in the Universe (Cambridge: Cambridge University Press)
Peebles, P. J. E. 1980, Large Scale Structure of the Universe (Princeton: Princeton University Press)
Pringle, J. E. 1981, A&AR, 19, 137
Ratra, B. 1992, ApJ, 391, L1
Rees, M. J., & Gunn, J. E. 1974, MNRAS, 167, 1
Rees, M. J., & Ostriker, J. P. 1977, MNRAS, 179, 451
Rees, M. J. 1984, A&AR, 22, 471
Rees, M. J. 1994, in Cosmical Magnetism, ed. D. Lynden-Bell (London: Kluwer)
Ruzmaikin, A. A., Shukorov, A. M., & Sokoloff, D. D. 1988, Magnetic Fields of Galaxies (Dordrecht: Kluwer)
Shakura, N. J., & Sunyaev, R. A. 1973, A&A, 24, 337
Shapiro, S. L., & Teukolsky, S. A. 1983, Black Holes, White Dwarfs and Neutron Stars (New York: Wiley)
Shlosman, I., Begelman, M. C., & Frank, J. 1990, Nature, 345, 679
Silk, J. I. 1977, ApJ, 211, 638
Silk, J. I., & Rees, M. J. 1998, A&A, 331, L1
Sellwood, J. A., & Moore, E. M. 1999, ApJ, 510, 125
Sellwood, J. A., & Balbus, S. A. 1999, ApJ, 511, 660
Subramanian, K. 1998, MNRAS, 294, 718
Sutherland, R., & Dopita, M. A. 1993, ApJS, 88, 253
Strom, R. G., & Duin, R. M. 1973, A&A, 25, 351
Spitzer, L. 1978, Physical Processes in the Interstellar Medium (New York: Wiley)
Toomre, A. 1964, ApJ, 139, 1217
Wandel, A. 1999, ApJ, 519, L39
White, S. D. M., & Rees, M. J. 1978, MNRAS, 183, 341